energy&fuels

pubs.acs.org/EF Article

Multiscale Catalytic Fast Pyrolysis of *Grindelia* Reveals Opportunities for Generating Low Oxygen Content Bio-Oils from Drought Tolerant Biomass

Phillip Cross,[⊥] Kristiina Iisa,[⊥] Anh To, Mark Nimlos, Daniel Carpenter, Jesse A. Mayer, John C. Cushman, Bishnu Neupane, Glenn C. Miller, Sushil Adhikari,* and Calvin Mukarakate*

Cite This: https://doi.org/10.1021/acs.energyfuels.1c02403 Read Online

ACCESS | Metrics & More | Article Recommendations | Supporting Information

ABSTRACT: *Grindelia squarrosa* (curlycup gumweed) biomass possesses unique biochemistry, cell wall composition, and leaf architecture tailored for prolific growth in arid and semiarid climates. Most notably, this plant has developed high levels of extractable resins that have high effective H/C_{eff} ratios ((mol H − 2 × mol O)/mol C), which is hypothesized to lead to low coke formation during catalytic fast pyrolysis (CFP) over the ZSM-5 catalyst. In microscale experiments with high ZSM-5 loadings (biomass-to-catalyst mass ratio (B/C) ∼ 0.1), *in situ* CFP generated high yields of aromatic hydrocarbons (30% carbon yield) while *ex situ* CFP favored aliphatic hydrocarbons (25% carbon yield). The difference between the two configurations was attributed to the constant catalyst temperature during *ex situ* CFP. Deactivation leading to partially deoxygenated vapor products occurred rapidly until B/C ≤ 0.5 by the adsorption of organic species blocking access to acid sites inside the micropores of the catalyst. This was followed by more gradual deactivation leading to primary vapor breakthrough, which we attribute to coke formation on acid sites on the external surface of ZSM-5 crystallites. Noncatalytic fast pyrolysis of *Grindelia* in a bench scale reactor produced oils with oxygen content (18 wt % on dry basis) and carbon yield (33%) comparable to those of CFP of woody biomass. The CFP of *Grindelia* further reduced the oxygen content to 7 wt % for *in situ* CFP and 4 wt % for *ex situ* CFP at B/C of 2−3. The good deoxygenation was attributed to a combination of a high H/C_{eff} ratio and overall better quality of the pyrolysis vapors that were passed over the ZSM-5 catalyst. The high inorganic content of the *Grindelia* likely catalyzed pyrolysis to remove oxygenated coke precursors. This integrated CFP study demonstrated that *Grindelia* could be an important feedstock for generating stabilized noncatalytic and CFP oils for downstream processing into fuels and/or extraction of high-value chemicals. The preprocessing of this feedstock will be required to remove inorganics, which cause an irreversible deactivation of ZSM-5.

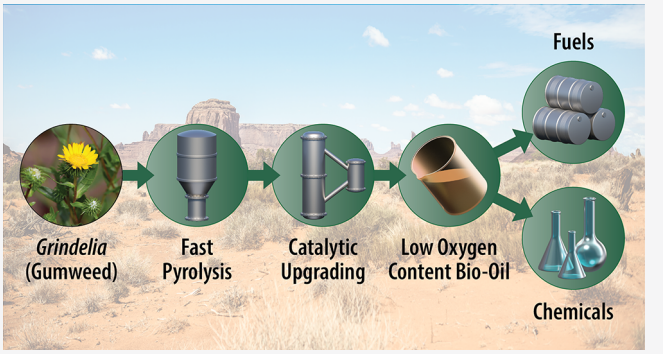

1. INTRODUCTION

The production of renewable fuels and chemicals from biomass is a key part of the U.S. strategy for reducing dependence on imported petroleum, improving air quality, and supporting rural economies. The large-scale use of nonfood biomass as a source of renewable carbon for fuels and chemicals will require the development of dedicated feedstocks co-optimized for growth and efficient conversion (high carbon and hydrogen retention, low catalyst deactivation). In the 21st century, we will see increased drought severity and duration through decreased precipitation/increased evaporation.[1,2] Therefore, drought-tolerant plants must be included in the biofuel economy. The benefits of drought-tolerant plants as feedstocks for biofuels and biochemicals have been identified by other groups[3,4] who stressed that increasing global temperature, drought, and soil-drying conditions caused by climate change will increase competition for agricultural freshwater and cultivated soils. Expanding available biomass resources to include plants with exceptional drought tolerance complements traditional lignocellulosic resources and has the advantage of lower water requirements and the use of arid and semiarid lands, potentially opening up large areas of the western U.S. to biofuel and biochemical production. The use of marginal lands with low water availability will be a crucial component to the success and ecological sustainability of a future bioeconomy.

Received: July 16, 2021
Revised: September 17, 2021

Biomass can be converted to fuels and chemicals *via* thermochemical methods, including by fast pyrolysis (heating to 400−600 °C in an inert atmosphere in the absence of added air or oxygen). Fast pyrolysis produces an oil, also called bio-oil or biocrude, that still contains significant amounts of oxygen, is corrosive, and is chemically unstable during storage and thermal processing.[5,6] The properties of the bio-oil can be improved by catalytic fast pyrolysis (CFP), which refers to upgrading the pyrolysis vapors over a catalyst prior to condensation. The higher-quality CFP oil can be further processed into fuels by coprocessing in refineries. The CFP catalyst can be placed directly in the pyrolyzer (*in situ* CFP) or in a separate upgrading reactor (*ex situ* CFP). Specifically, ZSM-5, a zeolite catalyst has been well-documented as a catalyst for CFP in both configurations.[7,8]

Grindelia (gumweed) was first identified as a biocrude-producing plant for arid climates in the 1980s.[9,10] A survey of 195 species conducted by McLaughlin et al. found that intermediate-sized plants that utilize less water than larger plants and produce unusually high yields of extractables make the most attractive species for producing bio-oil from drought-tolerant plants.[9] *Grindelia camporum* Greene was described as having these favorable characteristics. In later work, McLaughlin et al. emphasized that, in arid climates, biomass yield is not the main economic driver as yield is often tied to water use; instead, biomass quality, tied to the energy density of the resin, is the key parameter.[10] Biomass productivity estimates for curlycup gumweed (*Grindelia squarrosa*) range from 5.8 to 14.9 Mg ha^{-1}, with a mean of 9.9 Mg ha^{-1} resulting in the production of up to 1290 L ha^{-1} biofuel materials on a biennial basis.[11]

The resins of *Grindelia* have been an active area of research for decades and were well-summarized by Hoffman and McLaughlin.[12] There are an upward of 14 species of *Grindelia*, all producing unique compounds such as the essential oils borneol, terpineol, α-pinene, and β-pinene. All *Grindelia* species produce a set of primary compounds, labdane diterpene acids, including grindelic acid (2-[(2′*S*,4a*S*,8*R*,8a*S*)-2′,4,4,7,8*a*-pentamethylspiro[2,3,4*a*,5-tetrahydro-1*H*-naphthalene-8,5′-oxolane]-2′-yl]acetic acid) and its derivatives. These components pose an interesting opportunity for producing fuel through thermochemical conversion routes in that they have high effective H/C ratios (H/C$_{eff}$ defined as (mol H − 2 × mol O)/mol C) ranging from 1.3 to 1.8, as opposed to those of levoglucosan (H/C$_{eff}$ = 0) and guaiacol (H/C$_{eff}$ = 0.6), typical compounds found in woody biomass and agricultural residue pyrolysis products.[6] The H/C$_{eff}$ ratio is understood to be a critical aspect of CFP affecting coking.[13] High coking rates during CFP lead to both yield losses and rapid catalyst deactivation.[14] The reactivity of these primary vapors leads to thermally unstable pyrolysis oil that cannot be upgraded to finished fuels *via* hydroprocessing without significant fouling and plugging of reactors or multistage operation.[15,16]

The composition of pyrolysis vapors impacts the upgrading reactions over ZSM-5. The aromatic and alkene production cycles that occur on the zeolite catalyst have been found to behave differently depending on the H/C$_{eff}$ of the feed.[13] Zhang et al.[13] found that, in addition to reducing deactivation rates, increasing H/C$_{eff}$ increased the ratio of alkenes to aromatics during CFP of biomass. Ilias et al.[17] reported that cofeeding propene with dimethyl ether over ZSM-5 can increase the propagation of the alkene cycle, whereas cofeeding toluene can increase the aromatics cycle. These differences may have been also caused by the different H/C$_{eff}$ values for propene (2.0) and toluene (1.1).

Previous work conducted with *Grindelia* using noncatalytic fast pyrolysis at different temperatures determined several interesting characteristics of the fast pyrolysis vapors.[2] Most notable was the observation that the extractives were successfully volatilized at 450 °C and partially deoxygenated through thermal cracking at 550 °C, leading to the formation of aromatics and aliphatic hydrocarbons. The vapors produced from *Grindelia* during fast pyrolysis showed significant potential for application in the production of fuels due to the high fraction of hydrocarbons in the product and the consequent high H/C$_{eff}$ value. However, the oil yields may be low due to the high inorganics content of *Grindelia*, which leads to high char yields. To the best of our knowledge, these vapors have not been evaluated for CFP.

In this contribution, we show that the high H/C$_{eff}$ of *Grindelia* pyrolysis products leads to low catalyst deactivation during CFP and generates liquids with improved quality compared to standard clean pine feedstock. This was accomplished through integrated testing from microscale to bench scale, coupled with detailed catalyst characterization. The microscale studies enable the extraction of postreaction catalysts over a range of biomass vapor exposure levels (biomass-to-catalyst ratios) to evaluate deactivation, and the bench scale enabled us to obtain complete mass balances and characterize solid, gas, and liquid products. In addition, we evaluated the effect of catalyst placement (*in situ* vs *ex situ*) on CFP products.

2. EXPERIMENTAL SECTION

2.1. Feedstock and Catalyst Materials. *Grindelia squarrosa* (curlycup gumweed) was grown at the University of Nevada's research field plots. A description of the cultivation, preprocessing (drying and milling), and some characterization (proximate and ultimate analysis) of this feedstock can be found in previous publications by Neupane et al.[11] and Cross et al.[2] In short, *Grindelia* was dried to have 7−10% moisture content and milled using a hammer mill with a one-eighth inch screen. In the current work, *Grindelia* was characterized for volatiles, fixed carbon, moisture, and ash using ASTM D5142. Carbohydrates, lignin, proteins, and extractives were analyzed using the National Renewable Energy Laboratory's Laboratory Analytical Procedure.[18] Analysis of the inorganic ash elements was performed using inductively coupled plasma optical emission spectroscopy (ICP-OES). Samples were prepared *via* microwave assisted digestion using a CEM MARS 5 digester. Approximately 0.5 g of oil was digested in 10 mL of concentrated nitric acid. The microwave digester was operated at 1600 W and set to ramp to 200 °C in 15 min, holding at temperature for 15 min. After digestion, the samples were diluted to 50 mL with DI water and analyzed using an Agilent 5110 ICP-OES.

The ZSM-5 zeolite catalyst was obtained from Nexceris and was prepared by spray drying to obtain a particle size range of 300−500 μm. The catalyst uses an Al_2O_3 binder (boehmite, 10 wt %), and the ZSM-5 has a silica-to-alumina molar ratio (SAR) of 30.

2.2. Catalyst Characterization. Fresh and spent catalysts from the horizontal reactor−MBMS system were characterized for acid site density and strength, BET surface area, total pore volume, and coke content. Acid site density and strength were determined using ammonia-temperature-programmed desorption (NH_3-TPD), where the catalyst was first flushed with He (25 smL/min) at 120 °C for 2 h; NH_3 adsorption was performed at 120 °C for 30 min with 25 smL/min of 10% NH_3 in He and TPD at 120 °C for 1 h and then ramped at 30 °C min^{-1} to 500 °C and held for 1 h. N_2 physisorption isotherms were generated by first removing moisture at 150 °C under

https://doi.org/10.1021/acs.energyfuels.1c02403
Energy Fuels XXXX, XXX, XXX−XXX

He flow for 16 h, followed by N_2 physisorption at 77 K. BET surface area was calculated using $P/P_0 < 0.1$ and total pore volume at $P/P_0 > 0.995$. The amount and type of coke was determined using thermogravimetric analysis coupled to infrared analysis of gases (TGA-IR). One hundred milligrams of catalyst was placed in the TGA, and a gas flow of 25 smL/min N_2 was sent over the catalyst with a temperature ramp of 10 °C min^{-1} to 150 °C and held for 1 h to remove adsorbed moisture, followed by a 20 °C min^{-1} temperature ramp in 25 smL/min air to 800 °C. Detailed descriptions of the methods used for catalyst characterization and analysis are provided in the Supporting Information (SI).

2.3. Catalytic Fast Pyrolysis Reactor Systems. CFP was conducted on three different scales to determine pyrolysis chemistry, catalyst deactivation, and mass balances. The first reactor system was a tandem micro reactor coupled to a gas chromatograph mass spectrometer with a flame ionization detector and a thermal conductivity detector (py-GC-MS-FID-TCD) that used 0.5 mg biomass samples and 5 mg of catalyst. The GC-MS-FID-TCD product analysis equipment is well-suited for identifying and quantifying vapor phase products at low biomass-to-catalyst ratios (B/C = 0.1). The second reactor system was a horizontal quartz annular flow tube with a fixed catalyst bed coupled with a molecular beam mass spectrometer (py-MBMS). The py-MBMS uses 50 mg samples of biomass and 0.5−1 g of ZSM-5 and was used to evaluate deactivation by generating postreaction catalysts at various B/C ratios and optimize process conditions for use in the bench-scale reactor system. Lastly, the third reactor system was a bench-scale fluidized bed reactor, which feeds hundreds of grams of biomass over approximately 100 g of catalyst and produced enough product vapors to condense a liquid product for analysis and mass balance evaluation. Specific details of these reactor systems are given below.

2.3.1. Tandem Micro Pyrolyzer py-GC-MS-FID-TCD. Microscale experiments allow for the identification and quantification of volatile and semivolatile pyrolysis vapors. The microscale reactor was a Frontier Laboratories Rx-3050TR equipped with an autosampler (AS-1020E) and microjet cryo-trap (MJT-1030Ex). The GC unit (7890B, Agilent Technologies) was connected to a MS unit (5977A, Agilent Technologies) as well as an FID for vapor quantification and a TCD for light gas analysis. Parameters for the GC oven program, cryo-trap, and other details of the system can be found in a previous article.[19] For the pyrolysis reactor, the maximum heating rate of biomass is ∼500 °C s^{-1}.[20]

In situ CFP experiments were performed in triplicate; biomass samples of 0.5 mg were mixed with 5 mg of catalyst and loaded into small deactivated stainless-steel cups and charged into the first pyrolysis chamber set to 550 °C. During *ex situ* CFP experiments, 5 mg of catalyst was loaded into the second reactor chamber maintained at 550 °C, and 0.5 mg of biomass was charged into the first reactor chamber and the vapors were passed over the *ex situ* catalyst bed. Twenty biomass samples were charged over the same catalyst bed to evaluate changes in the vapor composition as a function of B/C.

Pyrolysis vapor compounds were identified using the NIST GC−MS library.[21] Carbon yield was calculated using a method similar to those described by Iisa et al.[22] and Xu et al.[23] The retention times of the compounds identified by MS were used to determine the corresponding FID peaks. Seventeen compounds were used to generate mass-based linear calibration curves to compile FID response factors correlating the FID peak integration area to micrograms of carbon. The MS area was used for the quantification of CO_2, and the TCD area was used for the quantification of CO. The list of standards can be found in the Supporting Information (SI). The carbon in noncalibrated compounds was determined using the normalization method where the response factor from a compound with the closest structure was used and the relative response factor was set to 1.[22,24]

2.3.2. Horizontal Fixed Bed Reactor−MBMS. The laboratory-scale horizontal reactor with MBMS allows for larger amounts of biomass and catalyst to be tested. Additionally, the MBMS does not require time-intensive chromatography, so biomass pulses can be fed immediately after one another, simulating a more continuous process than the micro scale experiments do. This laboratory scale reactor system is well-described in publications by Mukarakate et al.[14,25−27] The reactor system consisted of a quartz annular flow tube reactor coupled with an MBMS, which allows 50 mg samples of biomass to be charged to the reactor zone upstream of the 0.5 g packed catalyst bed. Three experiments were conducted where biomass was sequentially pulsed into the reactor system until a B/C of 0.5, 1.5, and 3.0. The vapor compositions were continuously monitored during these experiments in order to evaluate catalyst deactivation, and the postreaction catalysts were collected for characterization. Principal component multivariate analysis was performed to identify correlated mass spectral peaks using the Unscrambler software from Camo Software AS. The method has been previously described.[14] The process conditions optimized in the microscale (py-GCMS-FID-TCD and py-MBMS) systems were then used in the bench-scale reactor.

2.3.3. Two Inch Fluidized Bed Reactor System (2FBR). The 2 inch FBR was used to continuously feed biomass and generate enough pyrolysis vapors to condense liquid products. Details of the reactor system can be found in previous publications.[22,28,29] The system consisted of a 5.1 cm inner diameter fluidized bed reactor, a cyclone for char separation, a hot gas filter, a 3.2 cm inner diameter fixed bed reactor, and a condensation system (air cooled condenser, electrostatic precipitator, dry ice trap, coalescing filter in water-ice, a second dry ice trap). Three experiments were performed: noncatalytic fast pyrolysis (FP) and *in situ* and *ex situ* upgrading over ZSM-5. The fixed-bed reactor was bypassed in the FP and *in situ* CFP experiments. The ZSM-5 catalyst was placed in the fluidized bed reactor for *in situ* upgrading and in the fixed-bed reactor for *ex situ* upgrading. The reactors were operated at 500 °C, and other experimental details are presented in Table 1. He fluidizing gas was used in the pyrolyzer during *ex situ* CFP to address pressure drop challenges with the fixed-bed reactor.

Table 1. Details of the Fluidized Bed Reactor System Experiments

	fast pyrolysis	*in situ* CFP	*ex situ* CFP
fluidized bed reactor solids	silica sand	ZSM-5	silica sand
solids mass, g	330	147	330
fixed bed reactor solids	by-passed	by-passed	ZSM-5
solids mass, g			80
fluidization gas	N_2	N_2	He
fluidization gas flow, sL/min[a]	14.0	14.0	9.7
N_2 purges, sL/min[a]	1.9	1.9	1.9
total gas flow, sL/min[a]	15.9	15.9	11.6
biomass feed rate, g/h	300	150	150
biomass fed, g	304	297	242
biomass/catalyst (B/C), g/g		2.0	3.0
time, h	1.0	2.0	1.6
WHSV[b], g biomass/(g cat h)		1.0	1.9

[a]Standard liter/min at 0 °C and 1 bar. [b]Weight hourly space velocity.

The composition of the hot vapors before the condensation train was monitored by a Dycor 2000 residual gas analyzer (RGA, a mass spectrometer), and the composition of the exit gases was measured by an Agilent Pro microgas chromatograph (μGC) for H_2, CO, CO_2, and C_{1-4} hydrocarbons. Additionally, gas bag samples were taken intermittently and analyzed offline by an Agilent 7890A-5975 gas chromatograph−mass spectrometer (GC−MS) for the analysis of other organic vapors. The liquid yields were determined from the mass gain in the condensation train, coke by the mass increase in the catalyst bed, char from the mass increase in the cyclone and the hot gas filter, and gases from the exit gas flow rate and the gas analysis. The liquids were analyzed for carbon, hydrogen, and nitrogen content by a LECO TruSpec analyzer, for water by Karl Fischer titration, and for composition by GC−MS on the Agilent 7890A-5975 GC−MS using a Restek Rtx-50 column and a maximum oven temperature of 290 °C. Details on the GC−MS analysis and a list of standards can be found in the Supporting Information (SI).

https://doi.org/10.1021/acs.energyfuels.1c02403
Energy Fuels XXXX, XXX, XXX−XXX

Table 2. Compositional Analysis of *Grindelia* Feedstock

carbohydrate/lignin analysis (wt %)		proximate/ultimate analysis (wt %)		ICP ash analysis (wt %)	
ash	10.06	moisture	7.3 ± 0.1	Al	0.03 ± 0.00
structural inorganics	3.76	volatiles	76.1 ± 1.7	Ca	1.22 ± 0.03
nonstructural inorganics	6.29	fixed carbon	10.5 ± 1.8	Fe	0.04 ± 0.01
total protein	4.14	ash	6.2 ± 0.9	K	2.04 ± 0.04
structural protein	3.15	carbon	44.9 ± 0.4	Mg	0.17 ± 0.00
nonstructural protein	0.99	hydrogen	6.5 ± 0.1	Mn	0.005 ± 0.000
sucrose	0.84	nitrogen	1.2 ± 0.0	P	0.28 ± 0.01
free glucose	0.40	oxygen (by difference)	41.2	S	0.18 ± 0.00
free fructose	0.76			Zn	0.005 ± 0.000
other water extractable	19.29			total	3.96 ± 0.05
ethanol extractives	10.24	H/C_{eff}, mol/mol	0.36		
lignin	10.86				
glucan	16.28				
xylan	8.04				
galactan	2.11				
arabinan	3.13				
acetyl	1.90				
total	88.06				

3. RESULTS AND DISCUSSION

3.1. Feedstock Characterization. *Grindelia squarrosa* was extensively characterized as illustrated in Table 2. The adaptation of this plant to harsh arid climates and alkaline soils is seen in its composition. Extractables make up 39 wt % of *Grindelia*; of these, ethanol extractives comprise 10 wt % and other water extractables (i.e., not sugars, proteins, or inorganics) are 19 wt %. As discussed by Hoffman et al.,[12] most of the extractives reside on the surface of the plant to limit transpiration. The accumulation of alkaline and alkaline earth elements was also notable with calcium and potassium contents of 1.2 and 2.0 wt %, respectively. The H/C_{eff} was 0.36.

3.2. Effect of Catalyst Bed Placement on Vapor Composition during Catalytic Fast Pyrolysis in the Micro Pyrolyzer. The unique pyrolysis vapors from Grindelia were upgraded in the py-GC-MS-FID-TCD using both *in situ* CFP and *ex situ* CFP configurations. These configurations differ in vapor residence time, temperature profile, and vapor concentration. The B/C ratio was 0.1 (0.5 mg of biomass, 5 mg of catalyst), and the reaction temperature was 550 °C. In addition, the results were compared to those for noncatalytic fast pyrolysis with the same amount of biomass but no catalyst.[2]

The carbon yields (g of C in product/g of C in feed) of products by compound type and carbon number are illustrated in Figure 1 and Figure S1 in the SI. Oxygenates were the largest compound group during the noncatalytic fast pyrolysis of *Grindelia* (with phenols, carbonyls, acids, and alcohols major oxygenate groups, Table S1 in the SI), but with contributions from hydrocarbons (5% carbon yield), including those with carbon numbers ≥5, as was reported earlier.[2] Aromatic hydrocarbons and low-carbon number aliphatics (mainly alkenes) were the largest product pools during CFP and can be selectively formed by altering catalyst placement. *In situ* CFP generated the highest yields of aromatic hydrocarbons (30% carbon yield, Figure S1), whereas *ex situ* CFP favored aliphatics (25% carbon yield, Figure S1); higher aromatic hydrocarbons and lower alkenes for the *in situ* configuration have been found for other feedstocks as well.[7] Independent of catalyst placement, the most abundant 1-ring aromatic

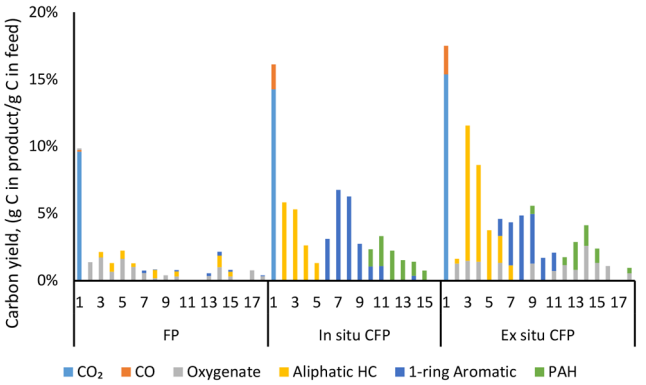

Figure 1. Carbon yields as a function of compound group and carbon number (*x* axis) in the py-GC-MS-FID-TCD experiments for fast pyrolysis (FP) and *in situ* and *ex situ* CFP (B/C 0.1).

hydrocarbons included toluene, xylene, and benzene (C_6–C_8 aromatic hydrocarbons, Figure 1, Tables S2 and S3). *In situ* CFP with *Grindelia* produced carbon yields of over 6% toluene, 6% xylenes, and 3% benzene and overall 15% carbon yield to BTX (benzene, toluene, and xylene), which exceeds values reported for *in situ* CFP of switchgrass (an overall BTX carbon yield of 10%).[30] This suggests that *Grindelia* could be a favorable feedstock for BTX production. Besides BTX, other polymethylbenzenes (1.8% C yield) and higher polymethyl aromatics, e.g., polymethyl naphthalene (6.7% C yield), were also observed in the product slate of *in situ* CFP of *Grindelia*. In contrast, continued growth of aromatics into 3-ring aromatics was low at 0.9% C yield. The polymerization of aromatic hydrocarbons to larger polycyclic aromatics is thought to lead to coke formation.[14,31,32] The low formation of three-ring aromatics with *Grindelia* was consistent with low coking rates.

The *ex situ* catalyst placement led to a more homogeneous catalyst temperature and longer contact/residence time, shifting the yields from aromatics to alkenes,[7] and the overall carbon yield of aromatics was lower for *ex situ* CFP than for *in situ* CFP (22 vs 30%, Figure S1). *Ex situ* CFP generated more aliphatic hydrocarbons whose total carbon yields were 25%

https://doi.org/10.1021/acs.energyfuels.1c02403
Energy Fuels XXXX, XXX, XXX−XXX

(Figure S1). *Ex situ* CFP selectively produced branched alkenes such as 2-methyl-2-butene compared to straight-chain alkenes like 1-butene (Table S3). Additionally, cyclic alkenes had a higher carbon yield for *ex situ* than *in situ* CFP. The carbon yields of alkenes for *Grindelia* were significantly higher than those reported by Wang et al.[7] for woody biomass (7.7%). *Grindelia* produced high carbon yields of C_3 (8.8%) and C_4 (7.1%) as well as C_5 (2.7%) and C_6 (2.3%) aliphatic hydrocarbons, whereas predominantly C_2 and C_3 alkenes have been reported for woody biomass at low B/C ratios.[7,32] The C_{5+} alkenes were also found in the noncatalytic *Grindelia* pyrolysis vapors though at lower concentrations. As discussed by Ilias et al.[17] and Zhang et al.,[33] increasing the H/C_{eff} ratio of the feedstock will increase the ratio of alkenes to aromatics in CFP products, which could explain the high alkenes for both CFP configurations for *Grindelia*.

The carbon yield to oxygenates was less than 1.0% from *Grindelia* with *in situ* CFP, whereas with *ex situ* CFP oxygenates comprised 9.5%. Higher yields of oxygenates with *ex situ* catalyst has been reported in other studies[28,34] and are typically attributed to the lower local vapor concentration and shorter residence times for *ex situ* CFP. The oxygenates from *Grindelia* included acetone, acetaldehyde, and furans plus a mixture of oxygenated one- and two-ring aromatic compounds with alcohol and carbonyl functional groups such as 6-(*p*-tolyl)-2-methyl-2-heptenol and 1*H*-inden-1-one, 2,3-dihydro-3,3,4,6-tetramethyl. These are presumed to be produced from the terpenoids and diterpenoids present in *Grindelia*.

The CO_2 carbon yields were high for all cases (close to 10% for noncatalytic FP and 14−15% for CFP) with low CO carbon yields (≤2% in all cases), which contrasts with other feeds, which typically produce more CO than CO_2.[7,30] The formation of CO_2 has been reported to correlate with the destruction of acids during CFP over ZSM-5,[35] and acids in *Grindelia* were high due to the presence of grindelic acid in extractives and acetic acid derived from acetyl groups (Table 2).

3.3. Vapor Composition as a Function of *ex Situ* Catalyst Deactivation. The shifts in pyrolysis vapor composition during *ex situ* CFP were determined using the py-GC-MS-FID-TCD system as well as the lab-scale horizontal quartz reactor with a MBMS detector. Biomass samples were introduced in the py-GC-MS-FID-TCD every 30 min to allow for the GC-oven to reach a programmed temperature of 300 °C and then cool to the initial temperature of 40 °C. The catalyst was assumed to maintain its functionality while being exposed to a hot He gas flow. In the py-MBMS experiments, biomass sample introductions were spaced by 1 min, which is more representative of continuous biomass feed. The multivariate analysis of the py-MBMS data (Figure 2) showed a principal component associated with hydrocarbons decreasing throughout the experiment, with a higher rate of decrease in the first half up to approximately B/C of 1. The hydrocarbons included *m*/*z* values consistent with aromatic hydrocarbons, e.g., *m*/*z* 78 benzene, 91/92 toluene, 106 xylenes, 142 methylnaphthalene, 156 dimethylnaphthalene, but also of alkenes (propene *m*/*z* 42). The partially upgraded vapors included peaks consistent with phenol (*m*/*z* 94), methyl phenol (*m*/*z* 108), dimethyl phenol (*m*/*z* 122), naphthol (*m*/*z* 144), methyl naphthol (*m*/*z* 158), and dimethyl naphthol (*m*/*z* 172), and they increased rapidly up to approximately B/C 0.5, after which they went through a shallow maximum. Primary vapors, in contrast, increased only slightly up to approximately B/C 0.5 after which they increased at a faster rate.

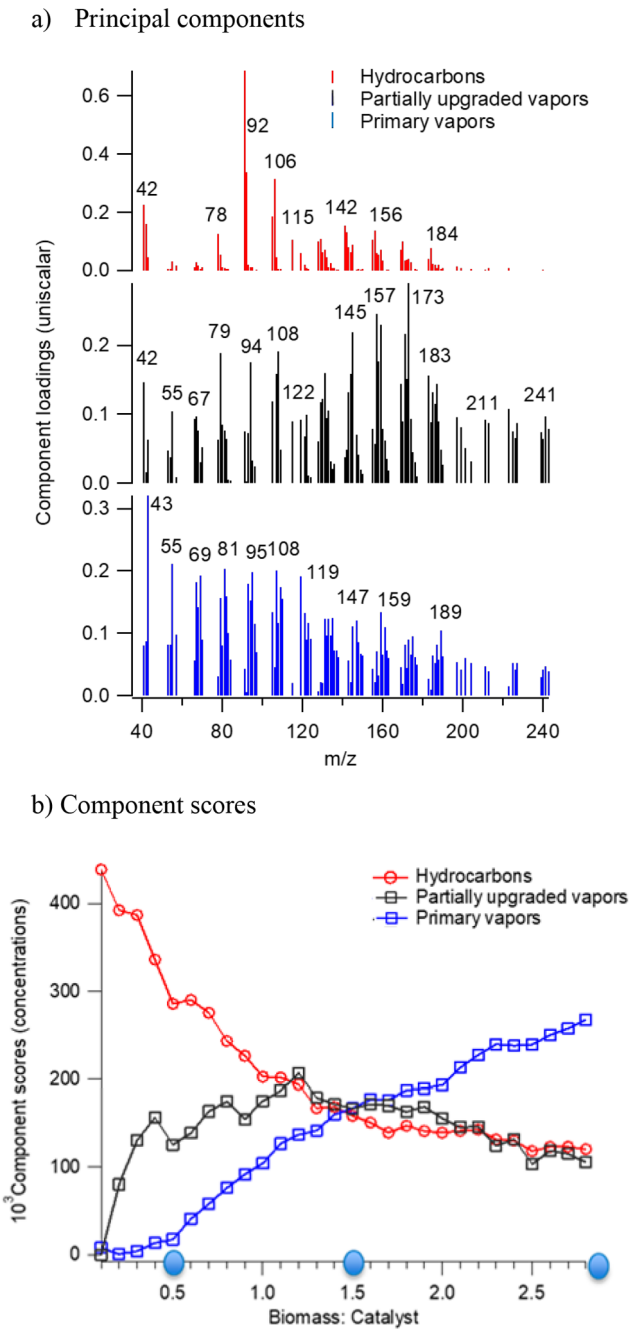

Figure 2. (a) Reconstructed spectra for pure components (PC 1−PC 3) from MCR-ALS analysis of upgrading gumweed vapors over ZSM-5, revealing changes in the composition of the product stream with catalyst deactivation. Note: the reconstructed spectra are unit-vector normalized. (b) Corresponding component scores from MCR-ALS analysis of vapor-phase upgrading experiment showing the dependency of each PC on B/C ratio. Spent catalysts were collected after running the *ex situ* CFP experiments to B/C of 0.5, 1.5, and 3.0.

Qualitatively similar results were obtained in the py-GC-MS-FID-TCD system, which enabled the identification of volatile and semivolatile vapors. Hydrocarbon yields decreased with an accompanying increase in oxygenates, partially upgraded vapors (here represented by furans, alcohols, carbonyls, and ethers), and primary vapors (here represented by acids and

https://doi.org/10.1021/acs.energyfuels.1c02403
Energy Fuels XXXX, XXX, XXX−XXX

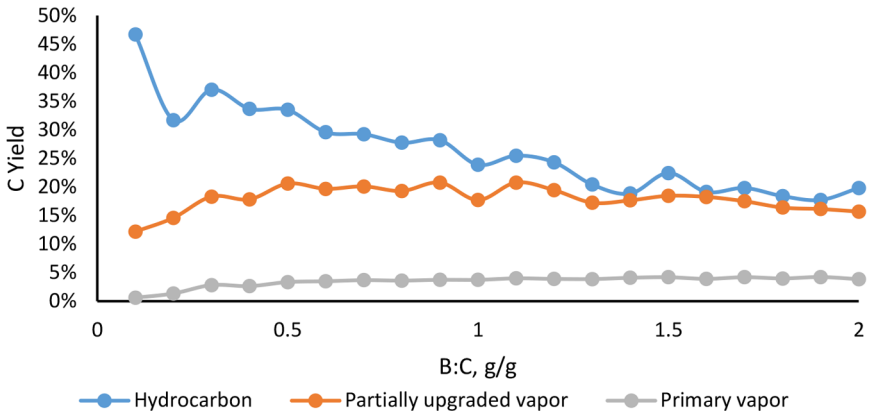

Figure 3. Fate of major compound groups during *ex situ* CFP of *Grindelia* up to B/C 2 in the py-GC-MS-FID-TCD system. Partially upgraded vapors include furans, alcohols, carbonyls, and ethers, and primary vapors include acids and esters.

Table 3. Summary of Coke Properties for Experiments Performed in py-MBMS

biomass	B/C (g biomass/g catalyst)	coke (g/g coked catalyst)	coke (g/g *Grindelia*)	total acid site density (mmol/g)	loss in acid site density	BET surface area (m^2/g)	BET surface area loss	total pore volume (cm^3/g)	total pore volume loss
				945		273		0.37	
Grindelia	0.5	1.6%	3.1%	491	48%	105	62%	0.16	57%
Grindelia	1.5	2.5%	2.5%	367[a]	61%	107	61%	0.16	57%
Grindelia	3.0	2.7%	1.8%	279	70%	109	60%	0.16	57%
Pine[14]	0.4	6.4%	17.1%				12%		27%
Pine[14]	1.0	7.8%	8.5%				19%		28%
Pine[14]	1.7	13.0%	8.8%				44%		43%
Pine[14]	5.0	15.5%	8.8%				67%		52%

[a]367 ± 15 range in duplicate measurement.

esters) (Figure 3). The partially upgraded vapors increased initially up to about B/C 0.5 but then became constant and slightly decreased.

The hydrocarbon species that were most abundant with the fresh *ex situ* catalyst were the most affected by the ZSM-5 deactivation. These included toluene and xylene within BTX, polymethylbenzenes, and small straight-chain alkenes (Figure S2a–c). Most of these compounds showed rapid deactivation after the first biomass pulse; however, by B/C 0.5, they were present in similar abundance to other hydrocarbons and their carbon yields decreased at a similar rate. The results suggest a decrease in the alkylation activity of the catalyst during the initial period up to B/C 0.5. The partially upgraded oxygenates increased in the same B/C frame (up to B/C 0.5) but remained relatively constant after that. The largest oxygenate group (Figure S2d) was carbonyls, which included high contributions of acetone, which was detected already at the lowest B/C of 0.1. The total yield of carbonyls did not return to the same level as during noncatalytic pyrolysis,[2] and this was reflected in the elevated CO levels throughout the deactivation experiments compared to noncatalytic fast pyrolysis (Figure 1, Figure S2e).

The trends from the MBMS agreed with the py-GC-MS-FID-TCD data, and collectively, both microscale results were used to determine the reaction conditions for the 2FBR bench-scale experiments (Table 1) discussed in Section 3.5.

3.4. Post-Reaction Catalyst Characterization. Changes in catalyst characteristics, including BET surface area and pore volume, acid site strength, and density, were evaluated for experiments performed at B/C of 0.5, 1.5, and 3.0 in the py-MBMS reactor (Table 3). Coke formation was significantly lower than for pine for similar experiments in the same system[14] with 3% coke on catalyst for *Grindelia* vs 13% for pine at B/C ∼ 1.5. The low coke values were consistent with the low formation of polyaromatic hydrocarbons in the py-GC-MS-FID-TCD. There may be several factors contributing to the lower coke yields of this drought-tolerant feedstock. One contributing factor is the higher H/C_{eff} for *Grindelia*.[33] The high levels of CO_2 in the noncatalytic pyrolysis vapors may also help to remove coke by converting it to CO.[36]

Despite the low coke values, there were significant decreases in acid site densities, BET surface area, and total pore volume (Table 3, Figure S3), and these were evident already for the first measurement point at B/C of 0.5. The N_2 physisorption isotherms (Figure S3a) suggested rapid decreases in the micropores, and the NH_3 profile (Figure S3b) showed decreases in the entire acid site strength range except for the very strongest acid sites. After B/C 0.5, the BET surface area and total pore volume stay approximately constant but the number of acid sites continued to decrease. A rapid decrease in hydrocarbons and a rapid increase in partially upgraded vapors can be seen up to B/C 0.5 (Figure 2b). B/C 0.5 also coincides with an increase in primary pyrolysis vapors. Compared to pine, the coke formation was low, but the decreases in surface area and pore volume were higher (Table 3).

ZSM-5 particles consist of small crystallites that are bound together with a binder, and the BET surface area includes both the external surface area of the crystallites (and the binder) and the micropore surface area, and similarly, the pore volume encompasses the micro pore volume and the volume between ZSM-5 crystallites and binder. We hypothesize that initially the entrances to micropores became blocked by the adsorption of

https://doi.org/10.1021/acs.energyfuels.1c02403
Energy Fuels XXXX, XXX, XXX−XXX

Grindelia vapor species, e.g., extractives (see the rapid initial loss in micropores in Figure S3a). The micropores may remain accessible to small molecules, such as N_2, but no longer for pyrolysis vapor. The acid sites with the highest strengths, which likely reside on the surfaces of ZSM-5 crystallites,[23] remained intact (Figure S3b). Continued upgrading led to very slow coke formation and a decrease in the number of acid sites but no appreciable changes in pore volume, BET surface area, or micropore volume. This trend with *Grindelia* was different from the trend observed with pine where coke deposition and pore blockage occurred concomitantly with increasing B/C ratios.[14] With pine, cellulose-derived vapors have been found to result in micropore blockage, whereas lignin produces coke on the external surface of the catalyst but does not block micropores.[32] Unlike pine, *Grindelia* has low cellulose and lignin contents but high extractives. This difference contributed to the distinctly different catalyst deactivation.

3.5. CFP Oil Yields and Composition in the Bench Scale. Experiments were performed in a bench-scale reactor system to produce CFP oils and obtain mass balance information. Table 4 compares *Grindelia* fast pyrolysis (FP) and CFP results to those for pine in the same reactor system at the same temperature.[28] The FP oil from *Grindelia* had a remarkably lower oxygen content, with only 18 wt % oxygen on dry basis (db) vs 36 wt % for pine, and it resembled the pine CFP oils with respect to oxygen content (Table 4). The carbon yield of *Grindelia* FP oil, while lower than the carbon yield of pine FP oil, was higher than that of pine CFP oil (33 vs 21−25%), which suggests that the fast pyrolysis of *Grindelia* could produce a stabilized bio-oil suitable for upgrading in oil refineries without further treatment.

Other significant differences compared to pine FP were a high H/C_{eff} (over 1 for *Grindelia* and 0.5 for pine) and high CO_2 yields as observed in the py-GC-MS-FID-TCD experiments (Figure 1) and high char yields (Table 4). *Grindelia* produced a high ash residue (6.2 wt %—Table 2—vs 0.3 wt % for pine in the reference experiments[28]), and the presence of inorganic constituents in the feed enhanced char formation.[37] CO_2 formation has been closely linked to acid destruction,[35] and grindelic acid and hemicellulose acetyl groups are likely sources for the high CO_2 formation for *Grindelia*.

The GC−MS analysis of the FP oil (Figure 4, Table S5) reveals the presence of fully or partially upgraded compounds, e.g., aliphatic hydrocarbons and phenolics without methoxy groups ("simple phenols"), relatively low contents of primary pyrolysis vapors, such as methoxyphenols, and no anhydro sugars. Typically for woody biomass FP, all detected compounds are oxygenates, including anhydro sugars and methoxyphenols, which are present in significantly higher concentrations than simple phenols are.[38] The sugar content in *Grindelia* was low (Table 2); in addition, inorganic components, e.g., alkaline and earth alkane metals, which were present in high abundance in *Grindelia*, are known to catalyze cellulose decomposition pathways that lead to the formation of small oxygenated molecules and char instead of anhydro sugars.[37,39] Accordingly, little or no anhydro sugars were detected in the FP oil, and furanics and carbonyls (ketones and aldehydes) were the main cellulose-derived compounds, and the char yield was high (Table 4). The presence of some minerals (NaCl, KCl, $MgCl_2$, and $CaCl_2$) has been reported to not have any impact on lignin pyrolysis apart from a small increase in char yield.[40] However, the similar measured concentrations of simple phenols compared to methoxyphenols suggests that the inorganic components in *Grindelia* catalyzed the deoxygenation of lignin monomers. The aliphatic hydrocarbons in the FP oil likely originate from the extractives, e.g., grindelic acid, which agrees with the high CO_2 yield.

Table 4. Yields and Oil Oxygen Content in Bench-Scale Experiments for Fast Pyrolysis and CFP of *Grindelia* and Pine

	Grindelia, this study			pine[28]		
	fast pyrolysis	*in situ*	*ex situ* (cat. in fixed bed)	fast pyrolysis	*in situ*	*ex situ* (cat. in fluid. bed)
biomass/catalyst, g/g	N/A	2.0	3.0	N/A	1.5	1.7
			yields, g/gfeed			
oil	22%	11%	10%	67%	17%	14%
aqueous	25%	27%	24%	N/A	25%	23%
gas	20%	24%	28%	18%	28%	28%
char	23%	20%	14%*	12%	10%	9%
coke	N/A	4.5%	1.5%	N/A	8.5%	7.2%
total	90%	86%	78%	97%	88%	82%
oil O content, wt % db	18%	7.2%	4.3%	36%	18%	16%
H/C_{eff}, mol/mol	1.06	1.04	1.08	0.51	0.73	0.76
			C yields, g of C/g of C in feed			
oil	33%	19%	19%	61%	25%	21%
aqueous	6%	3%	1%		3%	2%
gas	15%	21%	24%	18%	29%	28%
char	30%	26%	18%[a]	12%	14%	14%
coke	N/A	10.0%	3.3%	N/A	11%	12%
total	84%	79%	66%	91%	82%	77%
			gas yields, g/gfeed			
H_2	0.2%	0.1%	0.2%	N/A	0.1%	0.1%
CH_4	0.7%	0.4%	1.2%	1.4%	1.2%	1.5%
CO	3.0%	5.0%	4.1%	5%	16%	16%
CO_2	15%	13%	17%	8%	9%	9%
C_2-C_4	1.0%	4.9%	5.4%	1%	3%	2%

[a]Char yield likely erroneous (too low), leading to low mass balance closure. Char yields should be similar in all experiments.

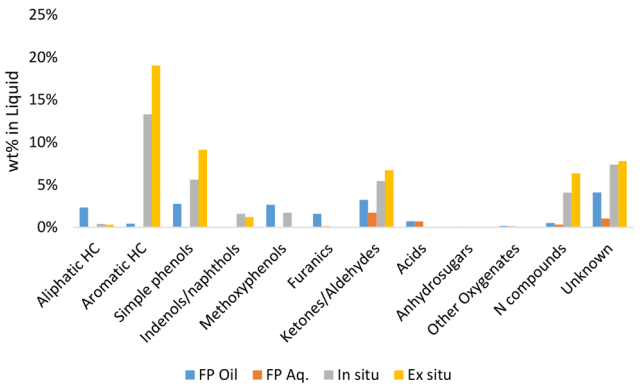

Figure 4. GC−MS analysis of liquids from the bench-scale *Grindelia* experiments by compound category. More details of the compounds at the highest concentrations are in Table S4.

https://doi.org/10.1021/acs.energyfuels.1c02403
Energy Fuels XXXX, XXX, XXX−XXX

The *Grindelia* CFP oils were highly deoxygenated: 7 and 4 wt % oxygen (db) for the *in situ* and the *ex situ* CFP oils, respectively (Table 4). Significantly lower oxygen contents were observed than for pine CFP (Table 4[28]), suggesting that the already partially deoxygenated pyrolysis vapors from *Grindelia* could be easily further upgraded over ZSM-5. While the FP oil carbon yield was significantly lower for *Grindelia* than for pine, the difference for CFP was much smaller (Table 4), and in particular, the carbon yield for *ex situ* CFP was remarkable (19% for CFP oil with 4 wt % oxygen) and suggests that CFP could be a viable process for producing hydrocarbons from *Grindelia*.

The *Grindelia ex situ* CFP oil had a lower oxygen content than the *in situ* CFP oil (4 vs 7 wt %) and a lower coke yield (1.5 vs 4.5%), which suggests slower deactivation for *ex situ* than *in situ* CFP. The lower coke formation for the *ex situ* configuration was in agreement with the lower polycyclic aromatics formation for the micropyrolyzer *ex situ* experiments (Figure 1). A higher polyaromatic formation for *in situ* than *ex situ* CFP has been previously reported for other feedstocks.[7,30] The nascent pyrolysis vapors in contact with the ZSM-5 catalyst in *in situ* CFP may be more prone to ring growth reactions than the vapors reaching the *ex situ* fixed bed reactor. Carlson et al.[31] concluded, on the basis of isotopic studies of glucose CFP, that naphthalene can be formed *via* a reaction involving oxygenated fragments from glucose or by a reaction between a monoaromatic and an oxygenate fragment. These oxygenate fragments may be more prevalent during *in situ* experiments, as the catalysts is in contact with pyrolysis vapors as they emerge from the biomass. Notably, the *Grindelia ex situ* oil had a lower oxygen content than the *in situ* oil despite the higher B/C ratio (3 vs 2 g/g) and the higher WHSV (1.9 vs 1.0 g biomass/(g catalyst h), Table 1). The *ex situ* upgrading was performed in a fixed bed reactor, whereas the *in situ* upgrading took place in a fluidized bed reactor. The contact between the vapors and the catalyst is better in a fixed bed than in a fluidized bed reactor, and this could have contributed to the observed very good deoxygenation in the *ex situ* configuration.

The contents of primary vapor compounds were very low in both *Grindelia* CFP oils, with no acids detected in either CFP oil and methoxyphenols only in the *in situ* CFP oil (Figure 4). The high deoxygenation was consistent with the high H/C_{eff} value for this biomass, which can lead to low catalyst coking and slow deactivation as hypothesized.[33] The GC−MS analysis confirmed the better deoxygenation for the *ex situ* experiment, showing a higher content of aromatic hydrocarbons and no methoxyphenols (Figure 4). The RGA traces also suggested a slower decay in the aromatic hydrocarbon signal for the *ex situ* than the *in situ* configuration (Figure S4).

The GC−MS analysis of the *Grindelia* CFP oils (Table S4) showed the presence of 2-ring aromatic hydrocarbons (e.g., naphthalenes), simple phenols (phenol and alkylphenols), naphthols, and N-containing compounds (e.g., indole and quinoline and their derivatives) in addition to carbonyls. The carbonyls included a compound tentatively identified as a tetramethylindanone present at a high concentration. This is a unique compound not typically identified in CFP oils and likely originates from the extractives in *Grindelia*. The identity and possible uses for this compound and other unidentified peaks with high GC−MS areas should be further evaluated.

The RGA traces from the CFP vapors (Figure S4) showed the intensities for aromatic hydrocarbon signals decaying during the catalytic experiment and those of partially upgraded vapors (e.g., m/z 68 for furan and 94 for phenol) increasing in accordance with the corresponding vapors in the horizontal fixed bed reactor-MBMS experiments (Figure 3). A primary vapor m/z of 60 (acetic acid or hydroxy acetaldehyde) was observed during pine CFP[28] but was nearly absent from the *Grindelia* RGA traces.

Overall, the results indicated that the more upgraded pyrolysis vapors from *Grindelia* than from pine led to a slower breakthrough of primary vapors during CFP. *Grindelia* also produced higher alkene yields than pine did (Table 4), in accordance with the anticipated impact of the higher H/C_{eff} ratio.[17,33]

Grindelia had high contents of several metals, including K and Ca (Table 2), which portioned mainly to the char fraction (Table S4). The large variation in the measured char metal contents was likely due to material inhomogeneity, but the fractions remaining in the char (calculated from char yields and the metals contents) suggested that some metals exited the pyrolysis bed with the vapors. The fraction remaining in the char was 50−85% for Ca and 45−76% for K, suggesting that significant fractions of K became volatilized or were carried *via* aerosols. The catalyst exposure to the metals will be different for the *in situ* and *ex situ* configuration and is expected to impact long-term catalyst poisoning. However, in these short-term experiments, the metals were unlikely to have had any major impact on the observed catalyst deactivation, which was more likely due to differences in coke formation by the pyrolysis vapors (contact with nascent pyrolysis vapors for *in situ* and more stabilized vapors for *ex situ* CFP).

4. CONCLUSION

The unique composition of the drought-tolerant *Grindelia* with high extractives and inorganics contents led to significant deoxygenation during noncatalytic fast pyrolysis, and the *Grindelia* fast pyrolysis oil resembled catalytic fast pyrolysis oil from woody biomass. The yields of *Grindelia* fast pyrolysis oils were also comparable to or higher than those from the catalytic fast pyrolysis of woody biomass. Thus, the fast pyrolysis of *Grindelia* affords an opportunity to obtain an upgraded oil *via* the much simpler fast pyrolysis process. The high effective hydrogen-to-carbon ratio of the pyrolysis vapors contributed to slow coking and catalyst deactivation during the CFP process, enabling the production of a catalytic fast pyrolysis oil with a very low oxygen content at a relatively high carbon yield. These opportunities (fast pyrolysis for upgraded oil and catalytic fast pyrolysis directly for hydrocarbon products) make *Grindelia* a promising alternative feedstock for the production of biofuels from biomass cultivated in arid lands. The impact of the high metals content on catalyst deactivation, opportunities for demineralization, and utilization of the compounds present in the oils at high contents should be further explored.

■ ASSOCIATED CONTENT

Supporting Information

The Supporting Information is available free of charge at https://pubs.acs.org/doi/10.1021/acs.energyfuels.1c02403.

Discussions of catalyst characterizations and GC−MS analysis, figures of distribution of gaseous and vapor products within major categories, carbon yield, N_2 physisorption isotherm, NH_3 desorption profile, and residual gas analyzer (RGA) traces, and tables of tandem microreactor compounds for fast pyrolysis of *Grindelia*,

https://doi.org/10.1021/acs.energyfuels.1c02403
Energy Fuels XXXX, XXX, XXX−XXX

metal contents in feedstock and char, and concentrations of main compounds in the liquid phase (PDF)

AUTHOR INFORMATION

Corresponding Authors

Sushil Adhikari − *Biosystems Engineering Department, Auburn University, Auburn, Alabama 36894, United States;* orcid.org/0000-0002-6539-6822; Email: sza0016@auburn.edu

Calvin Mukarakate − *Catalytic Carbon Transformation & Scaleup Center, National Renewable Energy Lab, Golden, Colorado 80401, United States;* orcid.org/0000-0002-3919-7977; Email: calvin.mukarakate@nrel.gov

Authors

Phillip Cross − *Biosystems Engineering Department, Auburn University, Auburn, Alabama 36894, United States*

Kristiina Iisa − *Catalytic Carbon Transformation & Scaleup Center, National Renewable Energy Lab, Golden, Colorado 80401, United States;* orcid.org/0000-0003-1326-901X

Anh To − *Catalytic Carbon Transformation & Scaleup Center, National Renewable Energy Lab, Golden, Colorado 80401, United States;* orcid.org/0000-0002-1594-1730

Mark Nimlos − *Catalytic Carbon Transformation & Scaleup Center, National Renewable Energy Lab, Golden, Colorado 80401, United States;* orcid.org/0000-0001-7117-775X

Daniel Carpenter − *Catalytic Carbon Transformation & Scaleup Center, National Renewable Energy Lab, Golden, Colorado 80401, United States;* orcid.org/0000-0001-7625-9308

Jesse A. Mayer − *Department of Biochemistry & Molecular Biology, MS330, University of Nevada, Reno, Nevada 89557-0330, United States*

John C. Cushman − *Department of Biochemistry & Molecular Biology, MS330, University of Nevada, Reno, Nevada 89557-0330, United States*

Bishnu Neupane − *Department of Natural Resource and Environmental Science, University of Nevada, Reno, Reno, Nevada 89557, United States*

Glenn C. Miller − *Department of Natural Resource and Environmental Science, University of Nevada, Reno, Reno, Nevada 89557, United States*

Complete contact information is available at: https://pubs.acs.org/10.1021/acs.energyfuels.1c02403

Author Contributions

⊥P.C. and K.I. contributed equally to the article.

Notes

The authors declare no competing financial interest.

ACKNOWLEDGMENTS

This work was authored by the National Renewable Energy Laboratory, operated by Alliance for Sustainable Energy, LLC, for the U.S. Department of Energy (DOE) under Contract No. DE-AC36-08GO28308. Funding was provided by U.S. Department of Energy Office of Energy Efficiency and Renewable Energy Bioenergy Technologies Office. This research was conducted in collaboration with the Chemical Catalysis for Bioenergy (ChemCatBio) Consortium, a member of the Energy Materials Network (EMN). The authors would like to thank Scott Palmer, Richard J. French, Kellene A. Orton, and Elizabeth Palmiotti at NREL for assistance with reactor operation and product analysis. The views expressed in this article do not necessarily represent the views of the DOE or the U.S. Government. The U.S. Government retains and the publisher, by accepting the article for publication, acknowledges that the U.S. Government retains a nonexclusive, paid-up, irrevocable, worldwide license to publish or reproduce the published form of this work, or allow others to do so, for U.S. Government purposes.

REFERENCES

(1) Dai, A. Increasing drought under global warming in observations and models. *Nat. Clim. Change* **2013**, *3*, 52.

(2) Cross, P.; Mukarakate, C.; Nimlos, M.; Carpenter, D.; Donohoe, B. S.; Mayer, J. A.; Cushman, J. C.; Neupane, B.; Miller, G. C.; Adhikari, S. Fast pyrolysis of Opuntia ficus-indica (prickly pear) and Grindelia squarrosa (gumweed). *Energy Fuels* **2018**, *32* (3), 3510−3518.

(3) Cushman, J.; Davis, S.; Yang, X.; Borland, A. Development and use of bioenergy feedstocks for semi-arid lands. *J. Exp. Bot.* **2015**, *66* (14), 4177−4193.

(4) Yang, X.; Cushman, J. C.; Borland, A. M.; Edwards, E. J.; Wullschleger, S. D. A roadmap for research on crassulacean acid metabolism (CAM) to enhance sustainable food and bioenergy production in a hotter, drier world. *New Phytol.* **2015**, *207* (3), 491−504.

(5) Bridgwater, A. V. Review of fast pyrolysis of biomass and product upgrading. *Biomass Bioenergy* **2012**, *38*, 68−94.

(6) Mohan, D.; Pittman, C. U.; Steele, P. H. Pyrolysis of Wood/Biomass for Bio-oil: A Critical Review. *Energy Fuels* **2006**, *20* (3), 848−889.

(7) Wang, K.; Johnston, P.; Brown, R. Comparison of in-situ and ex-situ catalytic pyrolysis in a micro-reactor system. *Bioresour. Technol.* **2014**, *173*, 124−131.

(8) Gamliel, D. P.; Du, S.; Bollas, G. M.; Valla, J. A. Investigation of in situ and ex situ catalytic pyrolysis of miscanthus x giganteus using a PyGC-MS microsystem and comparison with a bench-scale spouted-bed reactor. *Bioresour. Technol.* **2015**, *191*, 187−96.

(9) McLaughlin, S. P.; Hoffmann, J. J. Survey of Biocrude-Producing Plants from the Southwest. *Econ. Bot.* **1982**, *36*, 323−339.

(10) McLaughlin, S. P.; Kingsolver, B. E.; Hoffmann, J. J. Biocrude Production in Arid Lands. *Econ. Bot.* **1983**, *37* (2), 150−158.

(11) Neupane, B.; Shintani, D.; Lin, H.; Coronella, C.; Miller, G. Grindelia squarrosa: A Potential Arid Lands Biofuel Plant. *ACS Sustainable Chem. Eng.* **2017**, *5*, 995−1001.

(12) Hoffmann, J. J.; Mclaughlin, S. P. Grindelia camporum: Potential cash crop for the arid southwest. *Econ. Bot.* **1986**, *40* (2), 162−169.

(13) Zhang, H.; Cheng, Y.-T.; Vispute, T. P.; Xiao, R.; Huber, G. W. Catalytic conversion of biomass-derived feedstocks into olefins and aromatics with ZSM-5: the hydrogen to carbon effective ratio. *Energy Environ. Sci.* **2011**, *4* (6), 2297−2307.

(14) Mukarakate, C.; Zhang, X.; Stanton, A. R.; Robichaud, D. J.; Ciesielski, P. N.; Malhotra, K.; Donohoe, B. S.; Gjersing, E.; Evans, R. J.; Heroux, D. S.; Richards, R.; Iisa, K.; Nimlos, M. R. Real-time monitoring of the deactivation of HZSM-5 during upgrading of pine pyrolysis vapors. *Green Chem.* **2014**, *16* (3), 1444−1461.

(15) Elliott, D. C.; Hart, T. R.; Neuenschwander, G. G.; Rotness, L. J.; Olarte, M. V.; Zacher, A. H.; Solantausta, Y. Catalytic hydroprocessing of fast pyrolysis bio-oil from pine sawdust. *Energy Fuels* **2012**, *26* (6), 3891−3896.

(16) Mante, O. D.; Dayton, D. C.; Gabrielsen, J.; Ammitzboll, N. L.; Barbee, D.; Verdier, S.; Wang, K. Integration of catalytic fast pyrolysis and hydroprocessing: a pathway to refinery intermediates and "drop-in" fuels from biomass. *Green Chem.* **2016**, *18* (22), 6123−6135.

(17) Ilias, S.; Bhan, A. Tuning the selectivity of methanol-to-hydrocarbons conversion on H-ZSM-5 by co-processing olefins or aromatic compounds. *J. Catal.* **2012**, *290*, 186−192.

https://doi.org/10.1021/acs.energyfuels.1c02403
Energy Fuels XXXX, XXX, XXX−XXX

(18) Sluiter, A.; Hames, B.; Ruiz, R.; Scarlata, C.; Sluiter, J.; Templeton, D.; Crocker, D. *Determination of Structural Carbohydrates and Lignin in Biomass. Laboratory Analytical Procedure (LAP)*; National Renewable Energy Laboratory, 2012.
(19) Mukarakate, C.; Mittal, A.; Ciesielski, P.; Budhi, S.; Thompson, L.; Iisa, K.; Nimlos, M.; Donohoe, B. The influence of crystal allomorph and crystallinity on the products and behavior of cellulose during fast pyrolysis. *ACS Sustainable Chem. Eng.* **2016**, *4*, 4662.
(20) Proano-Aviles, J.; Lindstrom, J.; Johnston, P.; Brown, R. Heat and mass transfer effects in a furnace-based micropyrolyzer. *Energy Technol.* **2017**, *5*, 189−185.
(21) *2017 Mass Spectral Library, NIST MS Search version* 2.3; NIST, 2017.
(22) Iisa, K.; French, R.; Orton, K.; Budhi, S.; Mukarakate, C.; Stanton, A.; Yung, M.; Nimlos, M. Catalytic pyrolysis of pine over HZSM-5 with different binders. *Top. Catal.* **2016**, *59*, 94−108.
(23) Xu, M.; Mukarakate, C.; Iisa, K.; Budhi, S.; Menart, M.; Davidson, M.; Robichaud, D.; Nimlos, M.; Trewyn, B.; Richards, R. Deactivation of multilayered mfi nanosheet zeolite during upgrading of biomass pyrolysis vapors. *ACS Sustainable Chem. Eng.* **2017**, *5*, 5477−5484.
(24) Benkaci-Ali, F.; Baaliouamer, A.; Meklati, B.; Chemat, F. Chemical composition of seed essential oils from Algerian Nigella sativa extracted by microwave and hydrodistillation. *Flavour Fragrance J.* **2007**, *22*, 148−153.
(25) Murugappan, K.; Mukarakate, C.; Budhi, S.; Shetty, M.; Nimlos, M. R.; Román-Leshkov, Y. Supported molybdenum oxides as effective catalysts for the catalytic fast pyrolysis of lignocellulosic biomass. *Green Chem.* **2016**, *18* (20), 5548−5557.
(26) Mukarakate, C.; McBrayer, J. D.; Evans, T. J.; Budhi, S.; Robichaud, D. J.; Iisa, K.; ten Dam, J.; Watson, M. J.; Baldwin, R. M.; Nimlos, M. R. Catalytic fast pyrolysis of biomass: the reactions of water and aromatic intermediates produces phenols. *Green Chem.* **2015**, *17* (8), 4217−4227.
(27) Mukarakate, C.; Watson, M. J.; ten Dam, J.; Baucherel, X.; Budhi, S.; Yung, M. M.; Ben, H.; Iisa, K.; Baldwin, R. M.; Nimlos, M. R. Upgrading biomass pyrolysis vapors over β-zeolites: role of silica-to-alumina ratio. *Green Chem.* **2014**, *16*, 4891−4905.
(28) Iisa, K.; French, R. J.; Orton, K. A.; Yung, M. M.; Johnson, D. K.; ten Dam, J.; Watson, M. J.; Nimlos, M. R. In Situ and ex Situ Catalytic Pyrolysis of Pine in a Bench-Scale Fluidized Bed Reactor System. *Energy Fuels* **2016**, *30* (3), 2144−2157.
(29) Griffin, M. B.; Iisa, K.; Wang, H.; Dutta, A.; Orton, K. A.; French, R. J.; Santosa, D. M.; Wilson, N.; Christensen, E.; Nash, C.; Van Allsburg, K. M.; Baddour, F. G.; Ruddy, D. A.; Tan, E. C. D.; Cai, H.; Mukarakate, C.; Schaidle, J. A. Driving towards cost-competitive biofuels through catalytic fast pyrolysis by rethinking catalyst selection and reactor configuration. *Energy Environ. Sci.* **2018**, *11*, 2904−2918.
(30) Gamliel, D.; Du, S.; Bollas, G.; Valla, J. Investigation of in situ and ex situ catalytic pyrolysis of miscanthus x giganteus using PyGC-MS microsystem and comparison with a bench-scale spouted reactor. *Bioresour. Technol.* **2015**, *191*, 187−196.
(31) Carlson, T. R.; Jae, J.; Huber, G. W. Mechanistic Insights from Isotopic Studies of Glucose Conversion to Aromatics Over ZSM-5. *ChemCatChem* **2009**, *1* (1), 107−110.
(32) Stanton, A. R.; Iisa, K.; Mukarakate, C.; Nimlos, M. R. Role of Biopolymers in the Deactivation of ZSM-5 during Catalytic Fast Pyrolysis of Biomass. *ACS Sustainable Chem. Eng.* **2018**, *6* (8), 10030−10038.
(33) Zhang, H.; Cheng, Y.; Vispute, T.; Xiao, R.; Huber, G. Catalytic conversion of biomass-derived feedstocks into olefins and aromatics with ZSM-5: the hydrogen to carbon effective ratio. *Energy Environ. Sci.* **2011**, *4*, 2297−2307.
(34) Wan, S.; Wang, Y. A review on ex situ catalytic fast pyrolysis of biomass. *Front. Chem. Sci. Eng.* **2014**, *8* (3), 280−294.
(35) Patel, H.; Hao, N.; Iisa, K.; French, R. J.; Orton, K. A.; Mukarakate, C.; Ragauskas, A. J.; Nimlos, M. R. Detailed oil compositional analysis enables evaluation of impact of temperature and biomass-to-catalyst ratio on ex situ catalytic fast pyrolysis of pine vapors over ZSM-5. *ACS Sustainable Chem. Eng.* **2020**, *8*, 1762−1773.
(36) Liu, Z.; Nutt, M.; Iglesia, E. The effects of CO_2, CO and H_2 co-reactants on methane reactions catalyzed by Mo/H-ZSM-5. *Catal. Lett.* **2002**, *81*, 271−279.
(37) Trendewicz, A.; Evans, R.; Dutta, A.; Sykes, R.; Carpenter, D.; Braun, R. Evaluating the effect of potassium on cellulose pyrolysis reaction kinetics. *Biomass Bioenergy* **2015**, *74*, 15−25.
(38) Iisa, K.; French, R. J.; Orton, K. A.; Dutta, A.; Schaidle, J. A. Production of low-oxygen bio-oil via ex situ catalytic fast pyrolysis and hydrotreating. *Fuel* **2017**, *207*, 413−422.
(39) Patwardhan, P. R.; Satrio, J. A.; Brown, R. C.; Shanks, B. H. Influence of inorganic salts on the primary pyrolysis products of cellulose. *Bioresour. Technol.* **2010**, *101* (12), 4646−4655.
(40) Patwardhan, P. R.; Brown, R. C.; Shanks, B. H. Understanding the fast pyrolysis of lignin. *ChemSusChem* **2011**, *4* (11), 1629−1636.

https://doi.org/10.1021/acs.energyfuels.1c02403
Energy Fuels XXXX, XXX, XXX−XXX